A Finite Element Model for Structural and Aeroelastic Analysis of Rotary Wings with Advanced Blade Geometry

E. Piccione*, G. Bernardini and M. Gennaretti
University Roma Tre - Department of Mechanical and Industrial Engineering
* *Corresponding author:Via della Vasca Navale 79-00146 Rome, Italy, e-mail:epiccione@uniroma3.it*

Abstract: Objective of this paper is the development and implementation of a finite element model, in a Comsol Multyphisics context, for the prediction of the aeroelastic behavior of rotor blades. In particular, the attention is focused on new generation blades characterized by curved elastic axes, with the presence of tip sweep and anhedral angles. The blade structural model implemented is based on nonlinear flap-lag-torsion beam equations valid for slender, homogeneous, isotropic, non-uniform, twisted blades undergoing moderate displacements. Curved and arbitrarily oriented elastic axes are considered. A second-order approximation scheme for strain-displacement is adopted and inertial terms from rotating motion are included. For aeroelastic applications, aerodynamic loads are obtained from sectional theories, with inclusion of wake inflow models to take into account 3D effects. To validate the model implemented, several analyses are performed reproducing reliable results available in literature.

Keywords: innovative rotor blade geometry, rotor blade dynamics, rotor blade aeroelasticity.

1. Introduction

Rotary wing systems are frequently applied in aircraft. From the original application in single-rotor and tandem-rotor helicopters, nowadays they are used also in tiltrotor configurations. The main rotor plays a fundamental role in helicopter dynamics, and since early stages of the helicopter history has been carefully studied by researchers and manufacturer companies. Particular attention has been focused on the prediction of the aeroelastic behavior of the helicopter rotor blades, which requires the application of accurate structural and aerodynamic models. Helicopter rotor blades are flexible, light, slender structures and hence the structural model has to be able to take into account both the strong coupling between bending and torsion degrees of freedom and the nonlinearities arising from the significant deformations they usually experience.

One of the pioneering models for the description of the blade dynamics of pre-twisted nonuniform rotor blades was developed in Ref. [1], from a linear beam theory. Specifically, it presents the coupled equations governing in-plane bending (lag), out-of-plane bending (flap) and torsion of a twisted, rotating beam. More refined beam-like models for straight rotor blades have been developed in Refs. [2] and [3], where geometric nonlinearities are included in order to take into account moderate displacements of the blade. Aeroelastic applications of these structural models are presented in Refs. [4] and [5].

Next, models for new generation rotor blades with tip sweep and anhedral angles have been developed. One of the first structural models for swept tip rotor blades has been presented in Ref. [6], as a modification of a straight blade model by including the sweep effects as chordwise offsets of the center of gravity axis with respect to the (straight) elastic axis. However, this model has been proven to be not accurate [7, 8]. A structural model for swept blade tips has been presented and succesfully applied to hingeless rotor blades in Refs. [7, 8]. A formulation for blades with varying sweep, droop, twist, and planform is given in Ref. [9]. Ormiston and Hopkins [10] developed and validated a nonlinear finite element model for swept tip rotor blades considering large deflections. It is based on the theory by Hodges and Dowell [2], introducing a reference frame at the root of each beam element that is constrained to move with the tip node of the parent beam element (updated Lagrangian formulation). In this way, a sufficient number of beam elements enable the prediction of arbitrary large displacements. An experimental-theoretical investigation on the influence of tip sweep angle on the natural frequencies of vibrations of rotor blades is available

in Ref. [11].

Here, a nonlinear structural dynamic formulation suitable for analysis of blades having curved elastic axis is implemented in *Comsol Multyphisics*. It is an extension of the nonlinear flap-lag-torsion equations of motion presented in Ref. [2] for which each beam element is allowed to be arbitrarily oriented, thus permitting the simulation of tip sweep and anhedral angles effects. Numerical results will present a validation of the proposed *Comsol Multyphisics* application by comparison with experimental and numerical data available in the literature concerning free-vibration analysis of rotor blades with tip sweep and anhedral angles. In addition, coupling the structural dynamic model with a model predicting aerodynamic loads an aeroelastic formulation is developed in *Comsol Multyphisics* and the corresponding results are compared with literature data. The blade dynamics model implemented in *Comsol Multyphisics* is open to further improvements that could be focused both on the sophistication of the implemented structural/aerodynamic formulations and on the connection of the blade with rotor hub mechanics and control chain.

2. Blade structural model

In this work, the nonlinear equations for homogeneous, isotropic rotor blades with straight elastic axis undergoing moderate displacements presented in Ref. [2] are used as starting point to describe the structural dynamics of rotor blades with arbitrary shape of the elastic axis. Specifically, this is achieved by writing the elastic loads in terms of local variables along the (curvilinear) elastic axis, and developing general expressions for the inertial loads due to the rotary motion of the blades. In particular, the resulting formulation is suitable for the analysis of advanced geometry blades, like those with sweep and anhedral angles at the tip.

The equations implemented are obtained in a weak form, typical for finite element model, starting from Hamilton's principle

$$\delta I = \int_{t1}^{t2} \left[(\delta U - \delta T) - \delta W \right] dt = 0 \qquad (1)$$

where U is the strain energy, T is the kinetic energy, and δW is the virtual work of the external forces. The model includes spanwise variation in mass and stiffness properties, variable built-in pretwist, precone, sweep and anhedral angle. Nonlinear strain-displacement relationship are considered: second order terms are retained in the equations after the application of an ordering scheme that drops third-order terms (with respect to bending slope) not contributing to damping [2].

2.1 Variables and Coordinate Systems

Several coordinate systems are introduced to derive the equations of motion of the blade. The main ones, given in Fig. 1, are the rotating, hub-centered orthogonal system (x_R, y_R, z_R), the rotating, local, blade-fixed system, (x, y, z), with x axis aligned with the local undeformed elastic axis, and the rotating, local, blade-fixed system, (x', y', z'), with x' axis locally aligned with the elastic axis after deformation. Each beam finite element is defined through the local coordinate system (x, y, z). Deformations are described by displacements of the elastic axis and rotations of beam sections. Displacements, u, v, w, are defined in the local frames fixed with the undeformed blade, whereas the section rotation, ϕ, is about the x' axis.

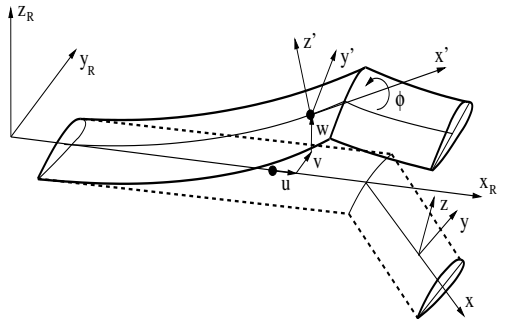

Figure 1: Undeformed and deformed blade configurations.

2.2 Strain energy contributions

The first variation of the strain energy appearing in Eq. (1) is given in terms of engineering stresses and strains as follows [2]

$$\delta U = \int_0^R \int_A (\sigma_{xx}\delta\epsilon_{xx} + \sigma_{x\eta}\delta\epsilon_{x\eta} + \sigma_{x\zeta}\delta\epsilon_{x\zeta})\, d\eta\, d\zeta\, dx$$

where R is the rotor radius, A denotes the section area, whereas η and ζ denote the principal cross section axes. Introducing the expressions for the engineering strain [2] into the equation above and assuming negligible cross-section

warping, the strain energy becomes

$$\delta U = \int_0^R \Big[V_{x'}(\delta u' + v'\delta v' + w'\delta w') + (S_{x'} + T_{x'})\,\delta\phi' + \Big(M_{z'}\cos\hat{\theta} + M_{y'}\sin\hat{\theta}\Big)(\delta v'' + w''\delta\phi) + \Big(M_{z'}\sin\hat{\theta} - M_{y'}\cos\hat{\theta}\Big)(\delta w'' - v''\delta\phi)\Big]\,dx \quad (2)$$

where $\hat{\theta} = \theta + \phi$, with θ denoting the blade cross-section pitch angle. In the equation above, neglecting higher order terms, stress resultants and moments are defined as [2]

$$\begin{cases} V_{x'} = EA\left(u' + \dfrac{v'^2}{2} + \dfrac{w'^2}{2} + k_A^2\theta'\phi'\right) \\ S_{x'} = GJ\phi' \\ T_{x'} = EAk_A^2\,\hat{\theta}\,'\left(u' + \dfrac{v'^2}{2} + \dfrac{w'^2}{2}\right) \\ M_{y'} = EI_{y'}\left(v''\sin\hat{\theta} - w''\cos\hat{\theta}\right) \\ M_{z'} = EI_{z'}\left(v''\cos\hat{\theta} + w''\sin\hat{\theta}\right) \end{cases}$$

In the equations above, E is the Young modulus, G is the shear modulus and

$$I_{z'} = \int_A \eta^2 d\eta d\zeta \qquad J = \int_A \left(\eta^2 + \zeta^2\right) d\eta d\zeta$$

$$I_{y'} = \int_A \zeta^2 d\eta d\zeta \qquad k_A^2 = \frac{1}{A}\int_A \left(\eta^2 + \zeta^2\right) d\eta d\zeta$$

Note that the blade cross sections have been assumed to be symmetric, and tensile and torque offsets have been assumed to be zero.

2.3 Kinetic energy contributions

The first variation of the kinetic energy appearing in Eq. (1) is given by

$$\delta T = \int_0^R \int_A \rho\,\vec{V}\cdot\delta\vec{V}\,d\eta\,d\zeta\,dx$$

where $\vec{V}$ denotes velocity of the blade points as observed by an inertial frame, and ρ is the density of the material. Expressing the blade velocity in terms of the variables introduced above, integrating by parts in time and over the blade cross section, δT becomes

$$\delta T = \int_0^R \left[(\bar{Z}_u + \bar{Z}_u^r)\,\delta u + (\bar{Z}_v + \bar{Z}_v^r)\,\delta v + (\bar{Z}_w + \bar{Z}_w^r)\,\delta w + (\bar{Z}_\phi + \bar{Z}_\phi^r)\,\delta\phi\right] dx \quad (3)$$

where

$$\begin{cases} \bar{Z}_u = -m\ddot{u} \\ \bar{Z}_v = -m\ddot{v} + me\ddot{\phi}\sin\theta \\ \bar{Z}_w = -m\ddot{w} - me\ddot{\phi}\cos\theta \\ \bar{Z}_\phi = -mk_m^2\ddot{\phi} + me\left[\ddot{v}\sin\theta - \ddot{w}\cos\theta\right] \end{cases}$$

while the $()^r$ terms due to the blade rotation will be given in the next section where, for the sake of clarity, they are derived from inertial loads directly written in terms of acceleration. In the equations above, m is the mass per unit length, e is the mass offset and mk_m^2 is the polar cross-section mass moment of inertia.

2.4 Inertial loads due to rotary motion

The expressions of the inertial loads due to the rotary motion of the blade are now obtained in the local, rotating, undeformed blade-fixed frame of reference. In order to take into account advanced blade geometry (including, for instance, tip sweep and anhedral angles), an elastic axis of arbitrary shape is considered in defining the kinematics of blade sections. The local acceleration due to blade rotation is given by

$$\vec{a} = \vec{\Omega}\times\vec{\Omega}\times\vec{r} + 2\,\vec{\Omega}\times\vec{v}$$

where $\vec{r}$ denotes the distance of a cross section point from the hub center, $\vec{v}$ is the velocity of the same point with respect to a rotating frame fixed with the undeformed blade, while $\vec{\Omega}$ is the blade angular velocity.

Then, considering components in the local blade-undeformed frame of reference, the resulting inertial distributed forces read

$$p_x = -\int_A \rho\,a_x\,d\eta\,d\zeta \qquad p_y = -\int_A \rho\,a_y\,d\eta\,d\zeta$$

$$p_z = -\int_A \rho\,a_z\,d\eta\,d\zeta$$

while the resulting inertial distributed moments defined with respect to the section shear center are given by

$$q_x = \int_A \rho\left[a_y(r_z - w) - a_z(r_y - v)\right] d\eta\,d\zeta$$

$$q_y = -\int_A \rho\left[a_x(r_z - w)\right] d\eta\,d\zeta$$

$$q_z = \int_A \rho\left[a_x(r_y - v)\right] d\eta\,d\zeta$$

Finally, the corresponding generalized inertial loads due to blade rotation appearing in Eq. (3) are obtained from the following combination of the distributed inertial loads [2]

$$\begin{cases} \bar{Z}_u^r = p_x \\ \bar{Z}_v^r = p_y - q_z' \\ \bar{Z}_w^r = p_z + q_y' \\ \bar{Z}_\phi^r = q_x + v' q_y + w' q_z \end{cases}$$

3. External aerodynamic loads

Aeroelastic applications of the blade structural model outlined in Section 2 require the introduction of the aerodynamic loads forcing the blade dynamics. Here, for the sake of simplicity, the aerodynamic loads are derived from a quasi-steady approximation of the Greenberg theory [12] for airfoils. Aerodynamic three-dimensional effects are taken into account by including a wake inflow model (see, for instance, Ref. [4] for details). Thus, section force, T, orthogonal to the chord, and section force, S, parallel to the chord are given by

$$T = \frac{\varrho\, C_{l_\alpha} c}{2}\left[-U_P U_T + \frac{c}{2}\,\omega\, U_T - \frac{c}{4}\dot{U}_P + \left(\frac{c}{4}\right)^2 \dot{\omega}\right]$$

$$S = \frac{\varrho\, C_{l_\alpha} c}{2}\left[U_P^2 - \frac{c}{2}\,\omega\, U_P - \frac{C_{d_0}}{C_{l_\alpha}} U_T^2\right]$$

while the section pitching moments with respect to the quarter-chord point reads

$$M_\phi = -\frac{\varrho\, C_{l_\alpha} c^3}{32}\left(\omega\, U_T - \dot{U}_P + \frac{3c}{8}\dot{\omega}\right)$$

In the equations above, U_P and U_T are, respectively, the quarter-chord velocity components normal and parallel to the chord after deformation, ω is the section angular velocity, c denotes the chord length, ϱ is the air density, C_{l_α} is the lift slope coefficient, while C_{d_0} is the drag coefficient.

Next, the blade aeroelastic equations are derived by expressing U_P, U_T and ω in terms of u, v, w and ϕ and expressing the aerodynamic forces given above, T and S, in terms of components, L_v and L_w, in the local blade undeformed frame of reference. Indeed, in Eq. (1) they contribute to the virtual work term as follows

$$\delta W = L_v\, \delta v + L_w\, \delta w + M_\phi\, \delta\phi \qquad (4)$$

4. Implementation in Comsol Multiphysics

The implementation in *Comsol Multiphysics* of both blade structural model and aerodynamic loads has been accomplished as a modification of the 3D Euler-Bernoulli beam model present in *Comsol Multiphysics 3.5a* Structural Mechanics package. This choice has been motivated mainly by the following two reasons: (i) the 3D Euler-Bernoulli beam model in *Comsol Multiphysics* has the same degrees of freedom of the rotating beam model to be implemented, and (ii) in the 3D Euler-Bernoulli finite element model transformations between global and local coordinate systems are automatically available. The model has been implemented replacing both *weak* and *dweak* terms appearing in the 3D Euler-Bernoulli beam model with those given in Eqs. (2) and (3), and defining all the parameters involved in them as global and local variables. Aerodynamic forces and moments appearing in Eq. (4) have been included as external distributed loads. The model implemented may be applied for static and dynamic solutions, as well as eigenvalue analysis.

5. Results

The aim of the numerical investigation is the validation of the finite element model implemented in *Comsol Multiphysics* in terms of both free-vibration analysis and aeroelastic response of a helicopter blade with sweep and anhedral angles at the tip (see Fig. 2). In particular, results from the present solver are compared with numerical and experimental data available in the literature.

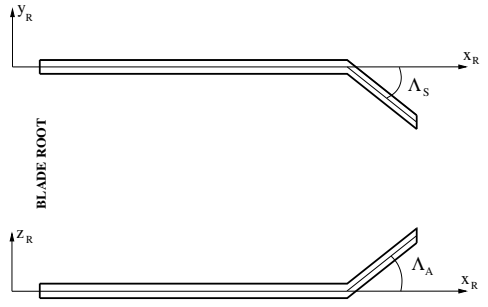

Figure 2: Blade tip sweep, Λ_S, and anhedral, Λ_A, angles.

5.1 In vacuo analyses

First, free-vibration, in-vacuo, analyses for the hingeless rotor blade model described in Ref. [10] are presented. Figures 3-5 show comparisons between present results and both numerical and experimental data given in Refs. [10] and [11], respectively. Specifically, Fig. 3 concerns the frequencies of vibration of the unswept rotating blade as functions of the rotating speed, Fig. 4 depicts the frequencies of vibration of the nonrotating blade for several values of the tip sweep angle (starting from the 85% of the blade span), while Fig. 5 shows the effects of the tip sweep angle on the frequencies of vibration of the rotating blade (note that, nondimensional frequencies and normalized rotation speed are related to the nominal blade rotating speed). For all the analyses presented the agreement of the present results with those from Refs. [10] and [11] is excellent, thus demonstrating the capability of the implemented finite element solver to capture the effects of rotation and curved elastic axis on free vibration of flap-lag-torsion beams. For instance, in the presence of swept tip, flap-torsion coupling is expected. Although not presented here, this behavior is correctly predicted by the present solver as revealed by observation of the predicted eigenvectors. In addition, also the significant effect of tip sweep angle on the torsional frequency experimentally observed for rotating blades (see Fig. 5) is well captured by the solver implemented in *Comsol Multiphysics*. These effects are a combination of centrifugal stiffening of 'tennis-racket' type with torsion first-mode inertia increase.

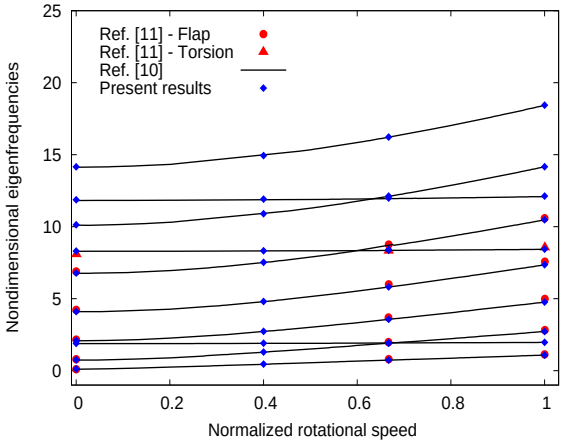

Figure 3: Normalized eigenfrequencies *vs* normalized rotor speed. Unswept blade.

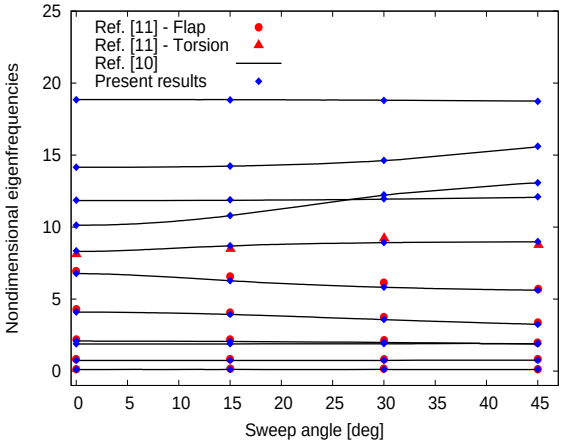

Figure 4: Normalized eigenfrequencies *vs* sweep angle. Nonrotating blade.

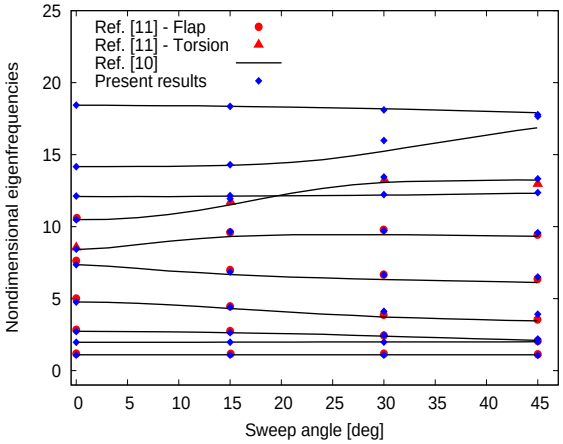

Figure 5: Normalized eigenfrequencies *vs* sweep angle. Rotating blade.

5.2 Aeroelastic analyses

Next some aeroelastic analyses for hovering configurations are presented for hingeless, straight rotor blades, as well as for hingeless rotor blades with tip sweep and anhedral angles.

First the untwisted, stiff-in-plane blade with straight elastic axis described in Ref. [4] is considered. Figure 6 depicts the steady-state deflections (flap-lag displacements and torsion rotation) at the tip of the blade, predicted for several values of the blade pitch angle. In addition, Figs. 7 and 8 present the results of the perturbation aeroelastic eigenanalysis (in terms of eigenfrequencies and dampings, respectively) carried out about the trim configuration of Fig. 6. Figures 6-8 show an excellent agreement between present results and those given in Refs. [4]

and [13] for the same rotor configurations, thus validating, for a straight blade, the formulation implemented in *Comsol Multiphysics*. These results demonstrate that the inclusion of aerodynamic effects introduces dampings in the blade dynamic behavior that are strongly dependent on the blade pitch (both directly and via the stationary trim configuration that is perturbed).

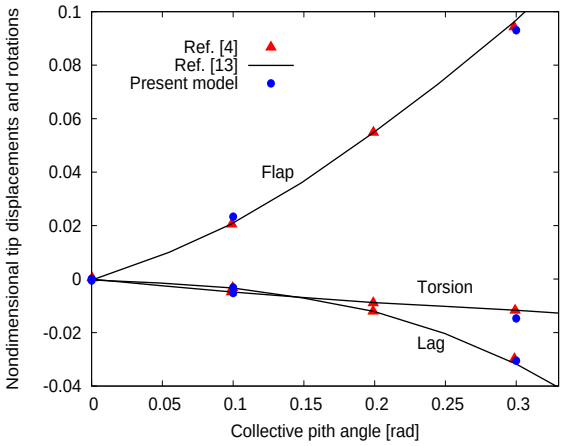

Figure 6: Equilibrium blade tip deflections.

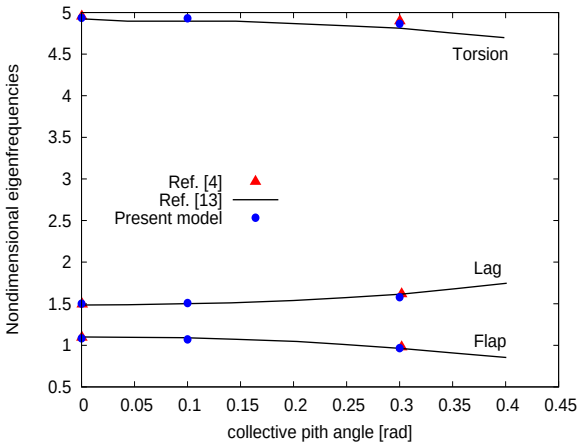

Figure 7: Aeroelastic eigenfrequencies for straight blade.

Then, the blade described in Ref. [13] is considered for the analysis on the aeroelastic stability effects due to tip sweep and anhedral angles. In particular, the tip 10% of the blade is subject to sweep and anhedral distortion. Figures 9 and 10 present the results of the aeroelastic eigenanalysis for the baseline blade given in Ref. [13] for several values of the sweep angle, respectively in terms of eigenfrequencies and

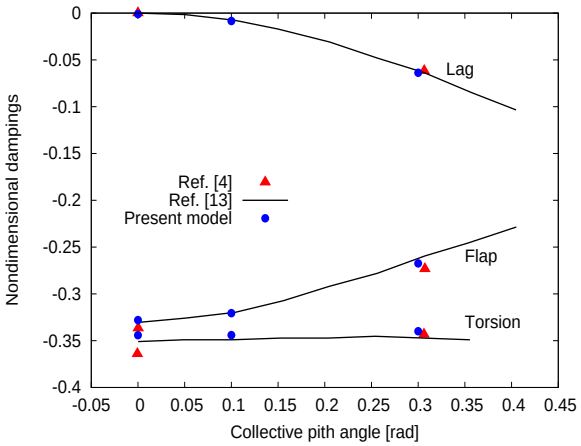

Figure 8: Aeroelastic dampings for straight blade.

dampings. Next, Figs. 11 and 12 show the same kind of results concerning a modified blade where structural data have been tailored so as to cause a strong coupling between first-torsion and second-flap modes. The comparison between the results presentd in Ref. [13] and those from the formulation implemented in *Comsol Multiphysics* reveals a very good agreement. In particular, the present approach is able to predict both the different influence the sweep angle has on the depicted modes and the instabilizing effects induced by the frequency coalescence appearing in the modified blade (see Figs. 11 and 12).

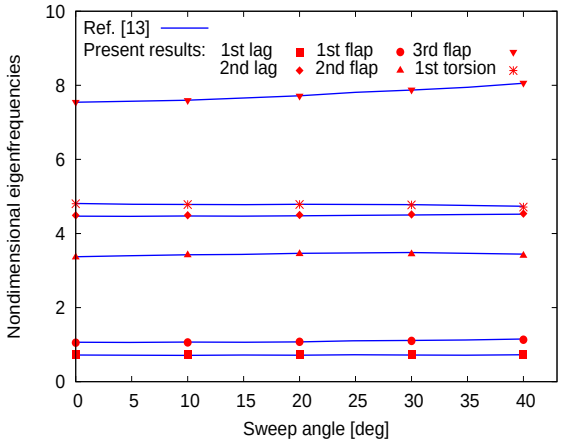

Figure 9: Aeroelastic eigenfrequencies *vs* sweep angle. Baseline blade.

Finally, the effects of anhedral angle on blade aeroelastic behavior has been investigated. Figures 13 and 14 show the results of the aeroelastic eigenanalysis for the baseline blade given

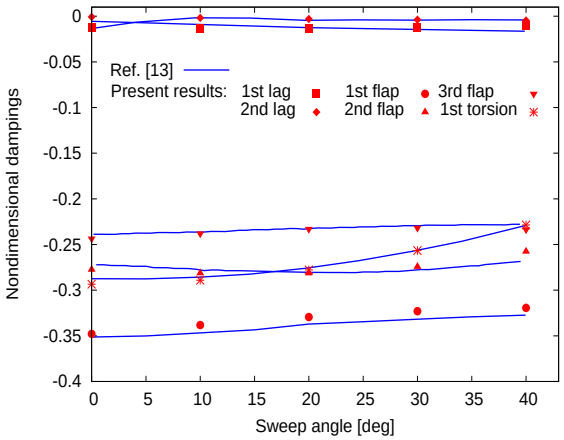

Figure 10: Aeroelastic dampings *vs* sweep angle. Baseline blade.

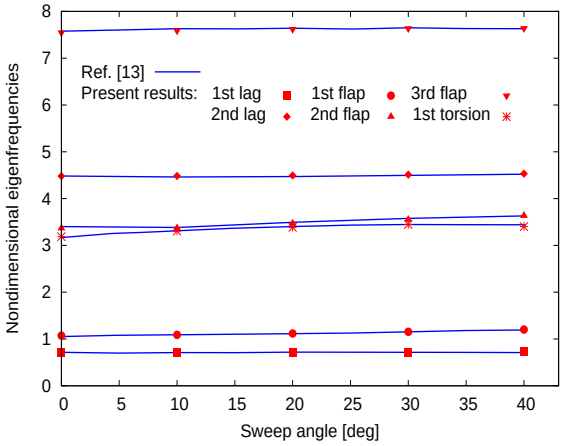

Figure 11: Aeroelastic eigenfrequencies *vs* sweep angle. Modified blade.

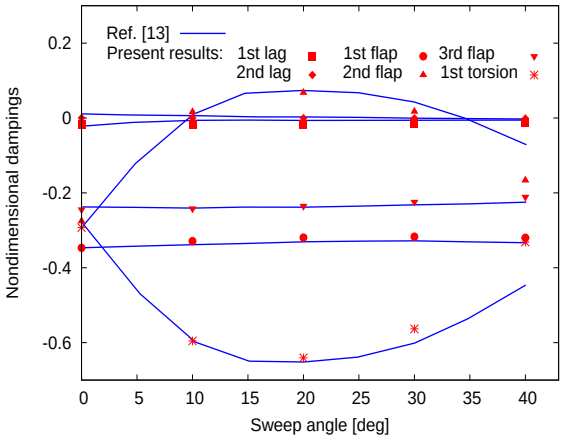

Figure 12: Aeroelastic dampings *vs* sweep angle. Modified blade.

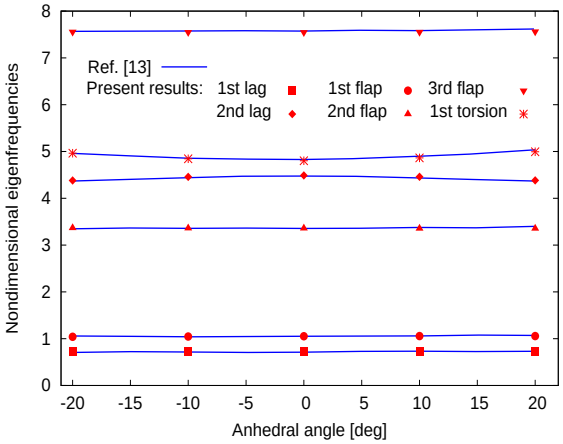

Figure 13: Aeroelastic eigenfrequencies *vs* anhedral angle. Baseline blade.

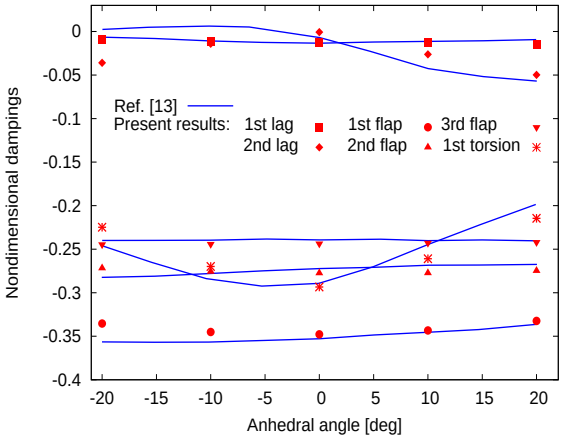

Figure 14: Aeroelastic dampings *vs* anhedral angle. Baseline blade.

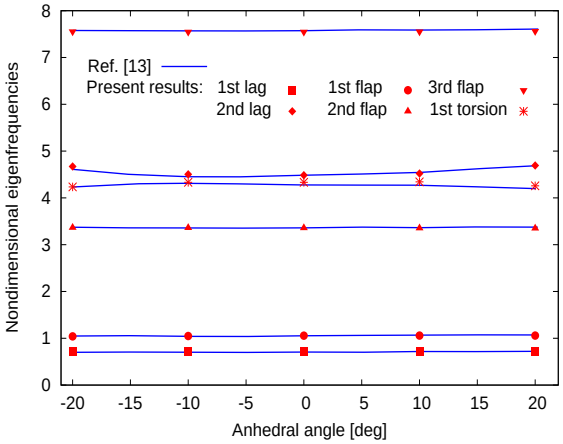

Figure 15: Aeroelastic eigenfrequencies *vs* anhedral angle. Modified blade.

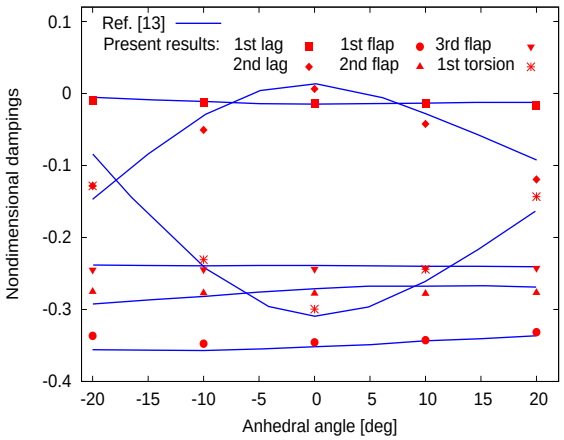

Figure 16: Aeroelastic dampings *vs* anhedral angle. Modified blade.

in Ref. [13], for several values of the anhedral angle, while Figs. 15 and 16 present the results of the same analysis concerning a modified balde model in which structural properties have been set to get the frequency coalescence between first-torsion and second-lag modes. Akin to the comparison presented for the sweep variation, the comparison between present results and those in Ref. [13] is quite good. The influence of anhedral angle on aeroelastic damping is well captured, as well as the instabilizing effects induced by the frequency coalescence appearing in the modified blade (see Figs. 15 and 16).

6. Conclusions

A nonlinear formulation for the structural and aeroelastic analysis of rotating blades with advanced geometry (nonuniform, twisted blades with curved elastic axis) has been implemented in the finite-element Structural Mechanics module of *Comsol Multiphysics*. It has been validated for both in-vacuo free-vibration analyses and hovering aeroelastic eigenanalyses, by comparison with experimental data and numerical results available in the literature. Both free-vibration and aeroelastic results have shown the capability of the formulation to predict with good accuracy the structural dynamics and aeroelastic behavior of rotating blades. In particular, structural coupling effects and influence of tip sweep and anhedral angles on aeroelastic damping have been shown to be correctly predicted. This validate the implemented blade model that seem to be a reliable tool for application in analysis and design of helicopter rotor blades and tiltrotor proprotors. Further developments include (from the structural point of view) the extension to non-isotropic blades and (from the aeroelastic point of view) the extension to forward flight configurations.

7. References

1. J.C. Houbolt and G.W. Brooks, Differential Equations of Motion for Combined Flapwise Bending, Chordwise Bending, and Torsion of Twisted Nonuinform Rotor Blades, *NACA Report 1346* (1958)
2. D.H. Hodges and E.H. Dowell, Nonlinear Equations of Motion for the Elastic Bending and Torsion of Twisted Nonuniform Rotor Blades, *NASA TN D-7818* (1974)
3. A. Rosen and P.P. Friedmann, The Nonlinear Behavior of Elastic Slender Straight Beams Undergoing Small Strains and Moderate Rotations, *Journal of Applied Mechanics*, **46**(1), 161-168 (1979)
4. D.H. Hodges and R.A. Ormiston, Stability of Elastic Bending and Torsion of Uniform Cantilever Rotor Blades in Hover with Variable Structural Coupling, *NASA TN D-8192* (1976)
5. J. Shamie and P.P. Friedmann, Effect of Moderate Deflections on the Aeroelastic Stability of a Rotor Blade in Forward Flight, *Procedings of 3rd European Rotorcraft and Powered Lift Aircraft Forum*, 24.1-24.37 (1977)
6. F.J. Tarzanin Jr. and R.R. Vlaminck, Investigation of the Effect of Blade Sweep on Rotor Vibratory Loads, *NASA-CR-166526* (1983)
7. R. Celi and P.P. Friedmann, Aeroelastic Modeling of Swept Tip Rotor Blades Using Finite Elements, *Journal of the American Helicopter Society*, **33**(2), 43-52 (1988)
8. R. Celi, Aeroelasticity and Structural Optimization of Helicopter Rotor Blades with Swept Tips, *PhD Dissertation*, Mechanical, Aerospace and Nuclear Engineering Department, University of California, Los Angeles (1987)
9. G.S. Bir and I. Chopra, Aeromechanical Stability of Rotorcraft with Advanced Geometry Blades, *Mathematical and Computer*

Modeling, **19**(314), 159-191 (1994)

10. A.S. Hopkins and R.A. Ormiston, An Examination of Selected Problems in Rotor Blade Structural Mechanics and Dynamics, *Proceedings American Helicopter Society 59th Annual Forum* (2003)
11. J.J. Epps and R. Chandra, The Natural Frequencies of Rotating Composite Beams With Tip Sweep, *Journal of the American Helicopter Society*, **41**(1), 29-36 (1996)
12. J.M. Greenberg, Airfoil in Sinusoidal Motion in Pulsating Stream, *NACA - TN 1326* (1947)
13. K.A. Yuan and P.P. Friedmann, Aeroelasticity and Structural Optimization of Composite Helicopter Rotor Blades With Swept Tips, *NASA CR-4665* (1995)